

Destabilizing turbulence in pipe flow

Jakob Kühnen^{1*}, Baofang Song^{1,2,3*}, Davide Scarselli¹, Nazmi Burak Budanur¹, Ashley Willis⁴, Marc Avila² and Björn Hof^{1†}

¹Nonlinear Dynamics and Turbulence Group, IST Austria, 3400 Klosterneuburg, Austria

²Center of Space Technology and Microgravity (ZARM), Universität Bremen, 28359 Bremen, Germany

³Center for Applied Mathematics, Tianjin University, No. 92 Weijin Road, Tianjin 300072, China

⁴School of Mathematics and Statistics, University of Sheffield, S3 7RH, United Kingdom

* These authors contributed equally to this work

†To whom correspondence should be addressed; bhof@ist.ac.at

Turbulence is the major cause of friction losses in transport processes and it is responsible for a drastic drag increase in flows over bounding surfaces. While much effort is invested into developing ways to control and reduce turbulence intensities¹⁻³, so far no methods exist to altogether eliminate turbulence if velocities are sufficiently large. We demonstrate for pipe flow that appropriate distortions to the velocity profile lead to a complete collapse of turbulence and subsequently friction losses are reduced by as much as 90%.

Counterintuitively, the return to laminar motion is accomplished by initially increasing turbulence intensities or by transiently amplifying wall shear. The usual measures of turbulence levels, such as the Reynolds number (Re) or shear stresses, do not account for the subsequent relaminarization. Instead an amplification mechanism^{4,5} measuring the interaction between eddies and the mean shear is found to set a threshold below which turbulence is suppressed beyond recovery.

Flows through pipes and hydraulic networks are generally turbulent and the friction losses encountered in these flows are responsible for approximately 10% of the global electric energy consumption. Here turbulence causes a severe drag increase and consequently much larger forces are needed to maintain desired flow rates. In pipes, both laminar and turbulent states are stable (the former is believed to be linearly stable for all Re, the latter is stable if $Re > 2040$ ⁶), but with increasing speed the laminar state becomes more and more susceptible to small disturbances. Hence in practice most flows are turbulent at sufficiently large Re. While the stability of laminar flow has been studied in great detail, little attention has been paid to the susceptibility of turbulence, the general assumption being that once turbulence is established it is stable.

Many turbulence control strategies have been put forward to reduce the drag encountered in shear flows⁷⁻¹⁷. Recent strategies employ feedback mechanisms to actively counter selected velocity components or vortices. Such methods usually require knowledge of the full turbulent velocity field. In computer simulations^{7,8} it could be demonstrated that under these ideal conditions, flows at low Reynolds number can even be relaminarized. In experiments the required detailed manipulation of the time dependent velocity field is, however, currently impossible to achieve.

Other studies employ passive (e.g. riblets) or active (oscillations or excitation of travelling waves) methods to interfere with the near wall turbulence creation. Typically here drag reduction of 10 to 40 percent has been reported, but often the control cost is substantially higher than the gain, or a net gain can only be achieved in a narrow Reynolds number regime.

Instead of attempting to control or counter certain components of the complex fluctuating flow fields, we will show in the following that by appropriately disturbing the mean profile, turbulence can be pushed outside its limit of existence and as a consequence the entire flow relaminarizes. Disturbance schemes are developed with the aid of direct numerical simulations (DNS) of pipe flow and subsequently implemented and tested in experiments. In the DNS a flow is simulated in a five diameter (D) long pipe and periodic boundary conditions are applied in the axial direction. Initially we perturb laminar pipe flow by adding fluctuation levels of a fully turbulent velocity field rescaled by a factor (k) to a laminar flow field. As shown in Fig.1a (dark blue curve), for small initial perturbations, i.e. small k , the disturbance eventually decays and the flow remains laminar. For sufficiently large amplitudes (k of order unity) turbulence is triggered (purple, red and cyan curves). So far this is the familiar picture of the transition to turbulence in shear flows, where turbulence is only triggered if perturbation amplitudes surpass a certain threshold. However, when increasing the turbulent fluctuations well beyond their usual levels ($k > 2.5$), surprisingly the highly turbulent flow almost immediately collapses and returns to laminar (light and dark green curves). Here the initially strong vortical motion leads to a redistribution of shear resulting in an unusually flat velocity profile (black profile in Fig.1c).

To achieve a similar effect in experiments we increase the turbulence level by vigorously stirring a fully turbulent pipe flow ($Re=3500$), employing four rotors located inside the pipe $50 D$ downstream of the pipe inlet (see supplementary movie 1 and Extended Data Fig. 1). As the highly turbulent flow proceeds further downstream it surprisingly does not return to the normal turbulence level but instead it quickly reduces in intensity until the entire flow is laminar (Fig.1 b top to bottom and supplementary movie 1). Being linearly stable the laminar flow persists for the entire downstream pipe. In a second experiment, turbulent flow ($Re=3100$) is disturbed by injecting fluid through 25 small holes (0.5mm diameter) in the pipe wall (holes are distributed across a pipe segment with a length of $25D$, (see Methods and Extended Data Fig.3)). Each injected jet creates a pair of counter-rotating vortices, intensifying the eddying motion beyond the levels of ordinary turbulence at this Re . The additional vortices redistribute the flow and as a consequence the velocity profile is flattened (Fig. 1c, purple dotted line). When the perturbation is actuated downstream fluctuation levels drop and the centre line velocity returns to its laminar value (Fig.1 d). Laminar motion persists for the remainder of the pipe. In this case the frictional drag is reduced by a factor of 2. Overall the injected fluid only amounts to $\sim 1.5\%$ of the total flow rate in the pipe. **With the present actuation device we achieved a net power saving (taking all actuation losses into account) of 32% over the remainder of the pipe. On the other hand the minimum actuation cost required to create the necessary flow disturbance is substantially lower ($\sim 1\%$), so that the net saving potential at this Re is 45% (see Methods).**

In another experiment we attempted to disrupt turbulence ($Re=5000$) by injecting fluid parallel to the wall in the streamwise direction (see Methods and Extended Data Fig. 2 and 4). Unlike for the previous case, this disturbance does not result in a magnification of cross-stream fluctuations, but instead **it directly** increases the wall shear stress and hence also the friction Reynolds number, Re_τ . Directly downstream of the injection point the latter is increased by about 15%. The acceleration of the near wall flow automatically causes deceleration of the flow in the pipe centre (the overall mass flux is held constant) hence again resulting in a flatter velocity profile (blue in Fig.1c). Despite the local increase in Re_τ , further downstream the fluctuation levels begin to drop and the turbulent flow has been sufficiently destabilized that eventually (30 D downstream) it decays and the flow returns to laminar. As a result, friction losses drop by a factor of 2.9 (see Fig.2a) **and the potential net power saving (not including actuation losses) is 55 %** (see Methods). For this type of perturbation we find, that relaminarization occurs for an intermediate injection range ($\sim 15\%$ of the flow rate in the pipe), while for smaller and larger rates the flow remains turbulent. A property common to all above relaminarization mechanisms is their effect on the average turbulent velocity profile.

In order to test a possible connection between the initial flat velocity profile and the subsequent turbulence collapse, we carried out further computer simulations where this time a forcing term was added to the full Navier Stokes equations. The force was formulated such that it decelerates the flow in the central part of the pipe cross section while it accelerates the flow in the near wall region. The mass flux through the pipe and hence Re remain unaffected (see Methods equ.3 and Extended Data Fig. 5). Unlike in the experiments where the disturbance is applied locally and persists in time, here the forcing is applied globally. As shown in Fig. 2b, upon turning on the forcing with sufficient amplitude the initially fully turbulent flow completely relaminarizes. Hence a profile modification alone suffices to destabilize turbulence. Interestingly, the energy required for the forcing is smaller than the energy gained due to drag reduction (even for intermediate forcing amplitudes Extended Data Fig.7). In this case we therefore obtain a net energy saving already in the presence of the forcing (in experiments the saving is achieved downstream of the perturbation location). After removal of the forcing (see Extended Data Fig.11) turbulence fluctuation levels continue to drop exponentially and the flow remains laminar for all times. This effect has been tested for fully turbulent flow for Reynolds numbers between 3000 and 100 000 and in all cases a sufficiently strong force was found to lead to a collapse of turbulence resulting in drag decrease and hence energy saving **in the numerical simulations** of up to 95% **(in practical situations finite amplitude perturbations may limit the persistence of laminar flow at such high Re)**.

We next investigate whether a profile modification on its own also relaminarizes turbulence in experiments. While body forces like that used in the simulations are not available (at least not for ordinary, non-conducting fluids), profiles can nevertheless be flattened by a local change in the boundary conditions. For this purpose one pipe segment is replaced by a pipe of slightly (4%) larger diameter which is pushed over the ends of the original pipe and can be impulsively moved

with respect to the rest of the pipe (see supplementary movie 2, Methods and Extended Data Fig. 5). The pipe segment is then impulsively accelerated in the streamwise direction and abruptly stopped, the peak velocity of the 300D long movable pipe segment is equal or larger (up to 3 times) than the bulk flow speed in the pipe. The impulsive acceleration of the near wall fluid leads to a flattened velocity profile (red profile in Fig. 1c). Despite the fact that overall the fluid is accelerated and additional shear is introduced (Re_τ is increased), after the wall motion is stopped (abruptly, over the course of 0.2 s) turbulence also in this case decays (see Fig. 2c and supplementary movie 2). If on the other hand the wall acceleration is reduced, with wall velocities lower than $0.8U$, turbulence survives. The impulsive wall motion is found to relaminarize turbulence very efficiently up to the highest Reynolds number ($Re=40\,000$) that could be tested in the experiment (here the wall was moved at the bulk flow speed).

In turbulent wall-bounded shear flows, energy has to be transferred continuously from the mean shear into eddying motion, and a key factor here is the interplay between streamwise vortices (i.e. vortices aligned with the mean flow direction) and streaks. The latter are essentially dents in the flow profile that have either markedly higher or lower velocities than their surroundings. Streamwise vortices “lift up” low velocity fluid from the wall and transport it towards the centre (see Extended Data Fig. 8). The low velocity streaks created in the process give rise to (nonlinear) instabilities and the creation of further vortices. Key to the efficiency of this “lift-up mechanism” is that weak vortices suffice to create large amplitude streaks. This amplification process is rooted in the non-normality⁴ of the linear Navier Stokes operator and its magnitude is measured by the so called transient growth (TG) (see also Extended Data Fig. 8 and 9).

Computing TG for the forced flow profiles in the DNS, we indeed observe that TG monotonically decreases with forcing amplitude (see Extended Data Fig. 10) and it assumes its minimum value directly before turbulence collapses. Generally, the flatter the velocity profile the more the streak vortex interaction is suppressed, and in the limiting case of a uniformly flat profile the lift up mechanism breaks down entirely.

Revisiting the experiments, the velocity profiles of all the disturbed flows considered exhibit a substantially reduced transient growth (Fig. 1c). For the streamwise injection, amplitudes relaminarizing the flow also show the minimum amplification (Fig. 2d) while at lower and higher injection rates where turbulence survives the amplification factors are higher and above the threshold found in the simulations. Similarly for the moving wall at sufficiently large wall acceleration where relaminarization is achieved, the lift up efficiency is reduced below threshold, while at lower wall speeds it remains above.

Some parallels between the present study and injection and suction control in channels and boundary layers^{18–20} can be drawn. While for boundary layers during the injection phase the drag downstream increases, during the suction it decreases. Suction applied to a laminar Blasius boundary layer leads to a reduction of the boundary layer thickness and this is well known to delay transition²¹ and push the transition location downstream.

The drag reduction achieved for the different methods used to destabilize turbulence is summarized in Fig.3. In each case the friction value before the profile modification corresponds to the characteristic Blasius law for turbulence (upper line) and after the disturbance it drops directly to the laminar Hagen-Poiseuille law. Hence the maximum drag reduction feasible in practice is reached (Fig.3b), and at the highest Reynolds numbers studied [in experiments](#), 90% reduction is obtained. Although the numerical and experimental relaminarization methods affect the flow in different ways, the common feature is that the velocity profile is flattened.

In summary we have shown that fully turbulent flow can be destabilized by appropriate perturbations. Unlike in previous control studies we do not target specific turbulent (e.g. near wall) structures but instead we distort the overall velocity profile. As a consequence the entire flow becomes laminar, drastically reducing friction losses. The commonly used criteria for flows to be turbulent, such as a threshold in the shear rate and the Reynolds number (see^{22,23} for other criteria) do not explain the collapse of turbulence observed here. Key to relaminarization is that the rearrangement of the mean turbulent profile inhibits the vortex streak interaction. As shown, this can be achieved in a variety of ways, offering a straightforward target for practical applications where potentially pumping and propulsion costs can be reduced by 95% or more. The future challenge is to develop and optimize methods that lead to the desired profile modifications in high Reynolds number turbulent flows.

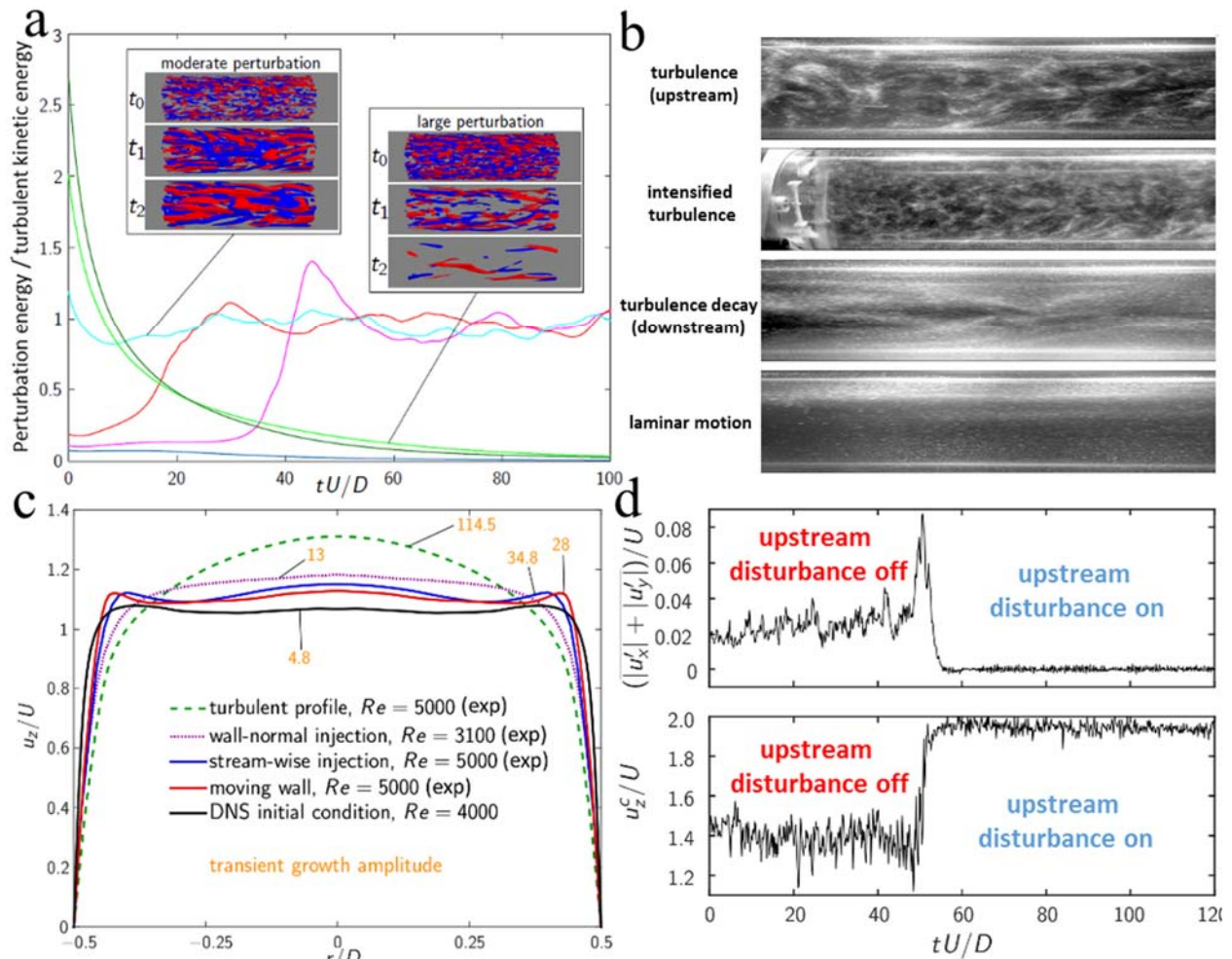


Fig. 1. Perturbing turbulence: **a** direct numerical simulations of pipe flow starting from turbulent initial conditions (taken from a run at $Re=10\,000$), rescaled by a constant factor k and added to the laminar base flow at $Re=4000$, which was then integrated forward in time (at $Re=4000$). For small initial energies perturbations die out (dark blue curve). For sufficiently large energies ($k \approx 1$) transition to turbulence occurs (red, purple, cyan). For even larger energies ($k > 2.5$) however the initially turbulent flow is destabilized and collapses after a short time (light and dark green curve). The 6 stream-wise vorticity isosurface figures show $\omega_z = \pm$ (red/blue) 7.2, 2.0, 1.6 U/D respectively at snapshot times $t_0 = 0$, $t_1 = 5$ and $t_2 = 10$ (D/U). **b** Fully turbulent flow (top panel) at $Re=3100$ is perturbed by vigorously stirring the fluid with four rotors. The more strongly turbulent flow (panel 2) eventually relaminarizes as it proceeds downstream (panel 3 and 4). **c** temporally and azimuthally averaged velocity fields of modified / perturbed flow fields in simulations and experiments. u_z is the streamwise velocity component, the cross stream components are denoted by u_r and u_θ . **d** Relaminarization of fully turbulent flow in experiments at $Re=3100$. The flow is perturbed by injecting 25 jets of fluid radially through the pipe wall. When actuated the fluctuation levels in the flow drop (top panel) and the centre line velocity switches from the turbulent level to the laminar value ($2U$, where U is the mean velocity in the pipe), bottom panel.

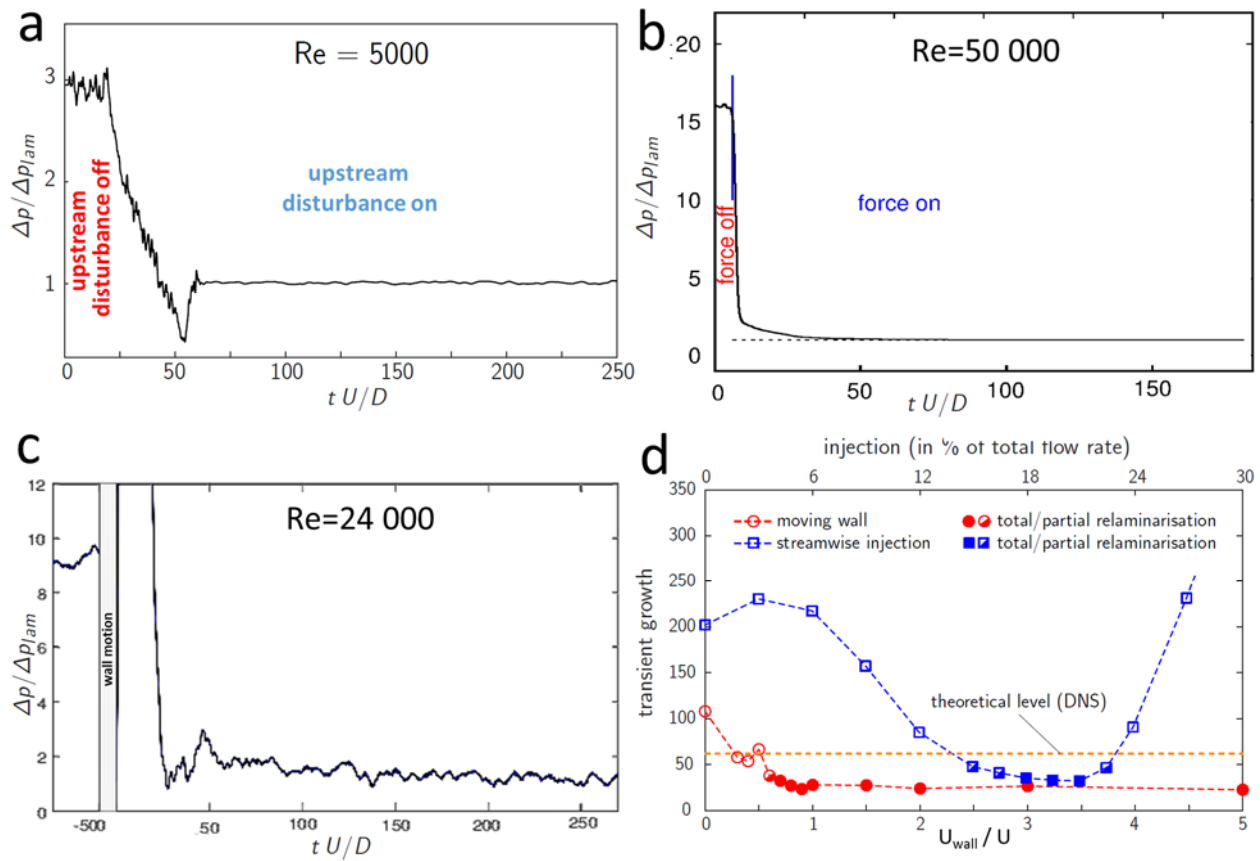


Fig. 2. Laminarization mechanisms. **a** After the streamwise near wall injection is actuated the pressure drop reduces to its laminar value. **b** A body force term is added in the numerical simulations which leads to an on average flatter flow profile (the fluid close to the wall is accelerated while it is decelerated in the near wall region). Disturbing the flow profile in this manner leads to a collapse of turbulence, here shown for $Re=50000$ where consequently friction losses drop by a factor of 10. **c** In the experiment the near wall fluid is accelerated via a sliding pipe segment, which is impulsively moved in the axial direction. Directly after the pipe segment is stopped the flow has a much flatter velocity profile. Subsequently turbulence collapses and the frictional drag drops to the laminar value. **d** Transient growth measures the efficiency of the lift up mechanism, i.e. how perturbations in the form of streamwise vortices are amplified while growing into streaks (deviations of the streamwise velocity component). All disturbance schemes used lead to a reduction in transient growth. The threshold value below which relaminarization occurs in the numerical (control via body force) is indicated by the orange line. For comparison the experimental flow disturbance mechanisms are shown in blue (streamwise injection) and red (moving wall). In agreement with the numerical prediction all disturbance amplitudes that lead to a collapse of turbulence (solid symbols) fall below the threshold value found in the simulations.

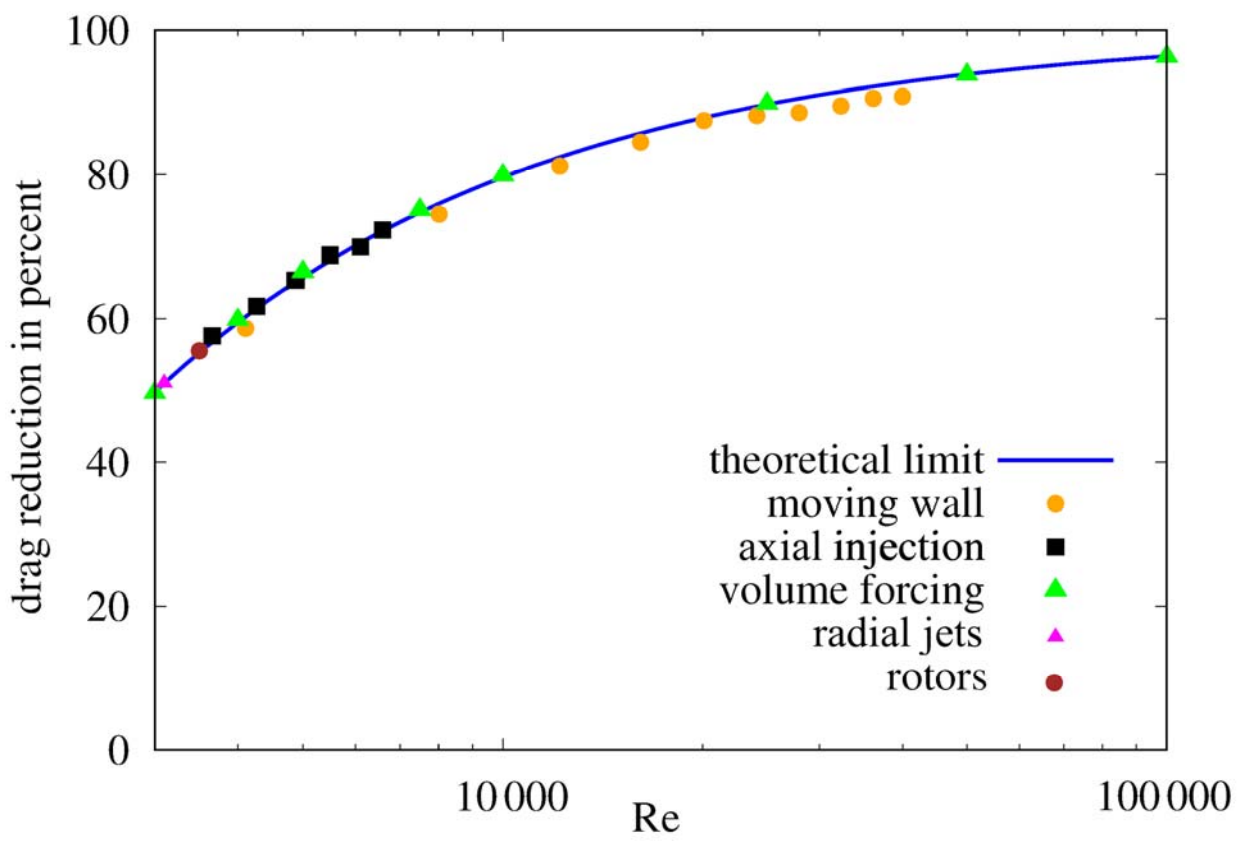
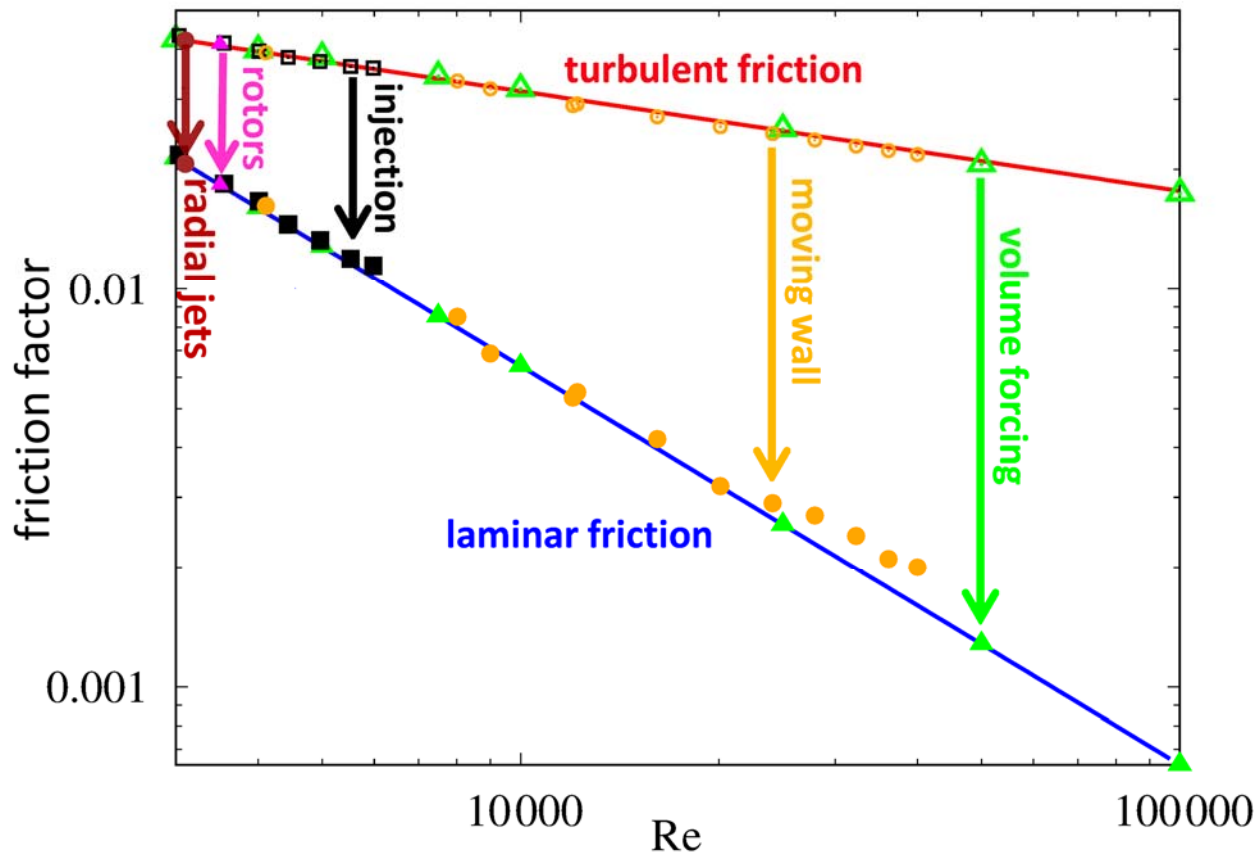


Fig. 3. Drag reduction. **a** Friction factor, f , as a function of Re . Initially all flows are fully turbulent and friction factors follow the Blasius-Prandtl scaling ($f=0.316 Re^{-0.25}$, red line). When the control is turned on flows relaminarize and the friction factors drop to the corresponding laminar values (Hagen- Poiseuille law in blue, $f=64/Re$). The rotors, radial jet injection, axial injection and moving wall controls- are carried out in laboratory experiments while the volume force cases are from direct numerical simulations of the Navier-Stokes equations. For all cases the Reynolds number is held constant throughout the experiment. **b** Drag reduction as a function of Re . For the injection perturbation a maximum drag reduction of $\sim 70\%$ was reached whereas for the moving wall and volume forcing 90 and 95% were achieved respectively. All data points reach the drag reduction limit set by relaminarization except for the $Re > 30000$ in experiments where values are slightly above. Although these flows are laminar (i.e. fluctuations are zero) the profile shape is still developing and has not quite reached the Hagen Poiseuille profile yet (the development length required to reach a fully parabolic profile increases linearly with Re).

1. Lumley, J. L. & Blossey, P. Control of turbulence. *Ann. Rev. Fluid Mech.* **30**, 311 (1998).
2. Kasagi, N., Suzuki, Y. & Fukagata, K. Microelectromechanical Systems – Based Feedback Control of Turbulence for Skin Friction Reduction. *Ann. Rev. Fluid Mech.* **41**, 231–253 (2009).
3. Kim, J. & Bewley, T. R. A Linear Systems Approach to Flow Control. *Ann. Rev. Fluid Mech.* **39**, 383–417 (2007).
4. Trefethen, L. N., Trefethen, A. E., Reddy, S. C. & Driscoll, T. A. Hydrodynamic stability without eigenvalues. *Science*. **261**, 578–584 (1993).
5. Brandt, L. The lift-up effect: The linear mechanism behind transition and turbulence in shear flows. *Eur. J. Mech. B/Fluids* **47**, 80–96 (2014).
6. Avila, K. *et al.* The onset of turbulence in pipe flow. *Science*. **333**, 192–196 (2011).
7. Bewley, T. R., Moin, P. & Temam, R. DNS-based predictive control of turbulence: an optimal benchmark for feedback algorithms. *J. Fluid Mech.* **447**, 179–225 (2001).
8. Högberg, M., Bewley, T. R. & Henningson, D. S. Relaminarization of $Re_{\tau}=100$ turbulence using gain scheduling and linear state-feedback control. *Phys. Fluids* **15**, 3572 (2003).
9. Auteri, F., Baron, a., Belan, M., Campanardi, G. & Quadrio, M. Experimental assessment of drag reduction by traveling waves in a turbulent pipe flow. *Phys. Fluids* **22**, (2010).
10. Lieu, B., Moarref, R. & Jovanovic, M. Controlling the onset of turbulence by streamwise travelling waves. Part 2. Direct numerical simulation. *J. Fluid Mech.* **663**, 100–119 (2010).
11. Moarref, R. & Jovanovic, M. Controlling the onset of turbulence by streamwise travelling waves. Part 1. Receptivity analysis. *J. Fluid Mech.* **663**, 70–99 (2010).
12. Quadrio, M., Ricco, P. & Viotti, C. Streamwise-traveling waves of spanwise wall velocity for turbulent drag reduction. *J. Fluid Mech.* **627**, 161–178 (2009).
13. Hof, B., De Lozar, A., Avila, M., Tu, X. Y. & Schneider, T. M. Eliminating Turbulence in Spatially Intermittent Flows. *Science*. **327**, 1491–1494 (2010).
14. Rathnasingham, R. & Breuer, K. Active control of turbulent boundary layers. *J. Fluid Mech.* **495**, 209–233 (2003).
15. Willis, A. P., Hwang, Y. & Cossu, C. Drag reduction in pipe flow by optimal forcing ' .
16. Du, Y. & Karniadakis, G. E. Suppressing Wall Turbulence by Means of a Transverse Traveling Wave. *Science*. **288**, 1230 (2000).
17. Min, T., Kang, S. M., Speyer, J. L. & Kim, J. Sustained sub-laminar drag in a fully developed channel flow. *J. Fluid Mech.* **558**, 309–318 (2006).
18. Park, J. & Choi, H. Effects of uniform blowing or suction from a spanwise slot on a

- turbulent boundary layer flow. *Phys. Fluids* **11**, 3095–3105 (1999).
19. Sumitani, Y. & Kasagi, N. Direct numerical simulation of turbulent transport with uniform wall injection and suction. *AIAA J.* **33**, 1220–1228 (1995).
 20. Fukagata, K., Iwamoto, K. & Kasagi, N. Contribution of Reynolds stress distribution to the skin friction in wall-bounded flows. *Phys. Fluids* **14**, 73–76 (2002).
 21. Fransson, J. H. M. & Alfredsson, P. H. On the disturbance growth in an asymptotic suction boundary layer. *J. Fluid Mech.* **482**, 51–90 (2003).
 22. Patel, V. C. & Head, M. R. Reversion of turbulent to laminar flow. *J. Fluid Mech.* **34**, 371–392 (1968).
 23. Yuan, J. & Piomelli, U. Numerical simulation of a spatially developing accelerating boundary layer over roughness. *J. Fluid Mech.* **780**, 192–214 (2015).